

# A new type of stellar explosion

H. B. Perets<sup>1</sup>, A. Gal-Yam<sup>1</sup>, P. Mazzali<sup>2,3,4</sup>, D. Arnett<sup>5</sup>, D. Kagan<sup>6</sup>,  
 A. V. Filippenko<sup>7</sup>, W. Li<sup>7</sup>, S. B. Cenko<sup>7</sup>, D. B. Fox<sup>8</sup>, D. C. Leonard<sup>9</sup>,  
 D.-S. Moon<sup>10</sup>, D. J. Sand<sup>11,12</sup>, A. M. Soderberg<sup>11</sup>, R. J. Foley<sup>11,13</sup>,  
 M. Ganeshalingam<sup>7</sup>, J. P. Anderson<sup>14,15</sup>, P. A. James<sup>15</sup>, E. O. Ofek<sup>16</sup>,  
 L. Bildsten<sup>17,18</sup>, G. Nelemans<sup>19</sup>, K. J. Shen<sup>18</sup>, N. N. Weinberg<sup>7</sup>,  
 B. D. Metzger<sup>7</sup>, A. L. Piro<sup>7</sup>, E. Quataert<sup>7</sup>, M. Kiewe<sup>1</sup>, and D. Poznanski<sup>7</sup>

<sup>1</sup> Faculty of Physics, Weizmann Institute of Science, POB 26, Rehovot 76100, Israel

<sup>2</sup> Max-Planck Institut fuer Astrophysik Karl-Schwarzschildstr. 1 85748 Garching, Germany

<sup>3</sup> Scuola Normale Superiore, Piazza Cavalieri 7, 56127 Pisa, Italy

<sup>4</sup> INAF - Oss. Astron. Padova, vicolo dell'Osservatorio, 5, 35122 Padova, Italy

<sup>5</sup> Steward Observatory, University of Arizona, 933 North Cherry Avenue, Tucson, AZ 85721, USA

<sup>6</sup> Department of Astronomy, University of Texas at Austin, Austin, TX 78712, USA

<sup>7</sup> Department of Astronomy, University of California, Berkeley, CA 94720-3411, USA

<sup>8</sup> Dept. of Astronomy and Astrophysics, Pennsylvania State University, University Park, PA 16802, USA

<sup>9</sup> Department of Astronomy, San Diego State University, San Diego, California 92182, USA

<sup>10</sup> Department of Astronomy and Astrophysics, University of Toronto, 50 St. George Street, Toronto, ON M5S 3H4,

Canada

<sup>11</sup> Harvard-Smithsonian Center for Astrophysics, 60 Garden Street, Cambridge, MA 02138, USA

<sup>12</sup> Las Cumbres Observatory Global Telescope, 6740 Cortona Dr. Ste. 102, Goleta, CA 93117, USA

<sup>13</sup> Clay Fellow

<sup>14</sup> Departamento de Astronomia, Universidad de Chile, Camino El Observatorio 1515, Las Condes, Santiago, Casilla 36-D,

Chile

<sup>15</sup> Astrophysics Research Institute, Liverpool John Moores University, Twelve Quays House, Birkenhead CH41 1LD, UK

<sup>16</sup> Department of Astronomy, 105-24, California Institute of Technology, Pasadena, CA 91125, USA

<sup>17</sup> Kavli Institute for Theoretical Physics, Kohn Hall, University of California, Santa Barbara, CA 93106

<sup>18</sup> Department of Physics, University of California, Santa Barbara, CA 93106

<sup>19</sup> Department of Astrophysics, Radboud University Nijmegen, Toernooiveld 1, NL-6525 ED, The Netherlands

---

The explosive deaths of stars (supernovae; SNe) are generally explained by two physical processes. Young massive stars (more than eight solar masses,  $M_{\odot}$ ) undergo gravitational core-collapse and appear as type Ib/c and II SNe. Type Ia SNe result from thermonuclear explosions of older, Chandrasekhar-mass carbon-oxygen white dwarfs (WDs).<sup>1</sup> Even the most underluminous SNe Ia<sup>2,3</sup> eject  $\sim 1 M_{\odot}$  of C/O burning products.<sup>4</sup> Here we report our discovery of the faint type Ib SN 2005E in the halo of the nearby isolated galaxy, NGC 1032. The lack of any trace of recent star formation near the SN location, and the very low ejected mass we find ( $\sim 0.3 M_{\odot}$ ) argues strongly against a core-collapse origin of this event (Fig. 1). Our spectroscopic

observations and the derived nucleosynthetic output show that the SN ejecta is dominated by helium-burning products, indicating that SN 2005E was neither a subluminous<sup>2</sup> nor a regular<sup>1</sup> SNe Ia (Fig. 2). We have therefore found a new type of stellar explosion, arising from a low-mass, old stellar system. The SN ejecta contain 5-10 times more calcium than observed in any known type of SNe,<sup>5,6</sup> and likely additional large amounts of radioactive <sup>44</sup>Ti. Such SNe may thus help resolve fundamental physical puzzles, extending from the composition of the primitive solar system and that of the oldest stars, to the Galactic production of positrons.

---

We discovered a supernova explosion (SN 2005E; Fig. 1) on Jan. 13, 2005 (UT dates are used throughout this paper) shortly after it occurred (it was not detected on Dec. 24, 2004). Follow-up spectroscopy (Fig. 2) revealed strong lines of helium and calcium, indicating it belongs to the previously identified group of calcium-rich type Ib supernovae.<sup>7</sup> The SN position is  $\sim 22.9$  kpc (projected) from the center and  $\sim 11.3$  kpc above the disk of its edge-on host galaxy, NGC 1032 (Fig. 1), which is itself at a distance of 34 Mpc. NGC 1032 is an isolated galaxy<sup>8</sup> showing no signs of interaction, with the closest small satellite galaxy found at a distance of  $> 120$  kpc in projection. Deep follow-up observations of the explosion site, sensitive to both ultraviolet light from hot young stars and emission lines from ionized hydrogen gas, put strict limits on any local star-formation activity at or near the SN location (Fig. 1). In addition, a radio signature, expected from some core-collapse SNe, has not been observed (see Supplementary Information [SI], Section 2). The remote position of SN 2005E in the outskirts (halo) of the galaxy, together with the isolation of NGC 1032 and its classification as an S0/a galaxy (in which the star-formation rate is very low<sup>9</sup>), in addition to our limits on local star formation, point to a SN progenitor from an old stellar population (see also SI, Section 2).

Our analysis of the spectra of SN 2005E indicates that it is spectroscopically similar to SNe Ib (Fig. 2; SI, Section 3), showing lines of He but lacking either hydrogen or the hallmark Si and S lines of SNe Ia in its photospheric spectra. The nebular spectrum of this event shows no emission from iron-group elements, which also characterize type Ia SNe. Analysis of this spectrum indicates a total ejected mass of  $M_{\text{ej}} \approx 0.2 M_{\odot}$ , with a small fraction in radioactive nickel, consistent with the low luminosity of this event (Fig. 3). Such low ejecta mass for a SN of any type has never before been firmly established using nebular spectral analysis. We also used the narrow, fast, and faint light curve together with the measured ejecta velocities ( $\sim 11,000 \text{ km s}^{-1}$ ) to infer the ejected mass (SI, Section 4). We use these data to find consistent results of  $M_{\text{ej}} \approx 0.3 \pm 0.1 M_{\odot}$ ,

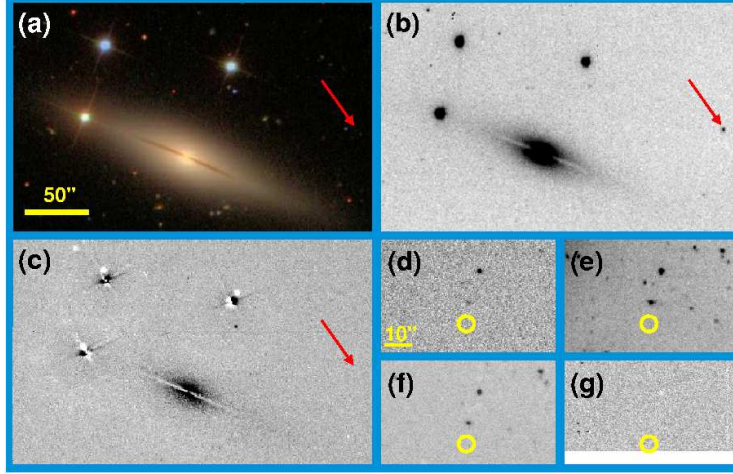


**Figure 1.** The environment of SN 2005E (technical details about the observations can be found in SI Section 1). **(a)** NGC 1032, the host galaxy of SN 2005E, as observed by the Sloan Digital Sky Survey (SDSS), prior to the SN explosion. The galaxy is an isolated, edge-on, early-type spiral galaxy, showing no signs of star-formation activity, warping, or interaction. Its luminosity is dominated by the cumulative contribution of a multitude of low-mass old stars (yellow light in this image). Panels **(a)**-**(c)** are  $275'' \times 175''$ ; a scale bar is provided, north is up, and east due left. **(b)** The LOSS<sup>10</sup> discovery of SN 2005E on Jan. 13, 2005 (shown in negative). Note the remote location of the SN (marked with a red arrow) with respect to its host, 22.9 kpc (projected) from the galaxy nucleus and 11.3 kpc above the disk, whose edge-on orientation is well determined (panel **(a)**). **(c)** An image of NGC 1032 in the light of the H $\alpha$  emission line, emitted by interstellar gas ionized by ultraviolet (UV) radiation, and a good tracer of recent star formation. There are no traces of recent star-formation activity (usually appearing as irregular, compact emission sources) near the SN location or anywhere else in the host. Panels **(d)**-**(g)** are  $64'' \times 36''$ ; a scale bar is provided. **(d)** Zoom-in on the location of SN 2005E in pre-explosion SDSS  $r$ -band images. No source is detected near the SN location, marked with a yellow circle (radius  $3''$ ; the astrometric uncertainty in the SN location is  $< 0.5''$ ). The SDSS catalog does not list any objects near that position (e.g., putative faint dwarf satellites of NGC 1032), down to a typical limit of  $r = 22.5$  mag. **(e-f)** Deeper photometry of the SN location. A red image is shown in panel **(e)**, while a UV ( $u$ -band) image is shown in panel **(f)**. At the distance of NGC 1032, the point source upper limits we find,  $M_r < -7.5(-6.9)$  and  $M_u < -8.1(-7.1)$  mag at  $3(2)\sigma$ , respectively, indicate that we would have detected faint star-forming galaxies or star-forming regions at the SN location, or indeed even individual massive red supergiant or luminous blue supergiant stars. **(g)** Zoom-in on the location of SN 2005E in H $\alpha$  light (see panel **(c)** for details). No trace of star-formation activity is seen near the SN location.

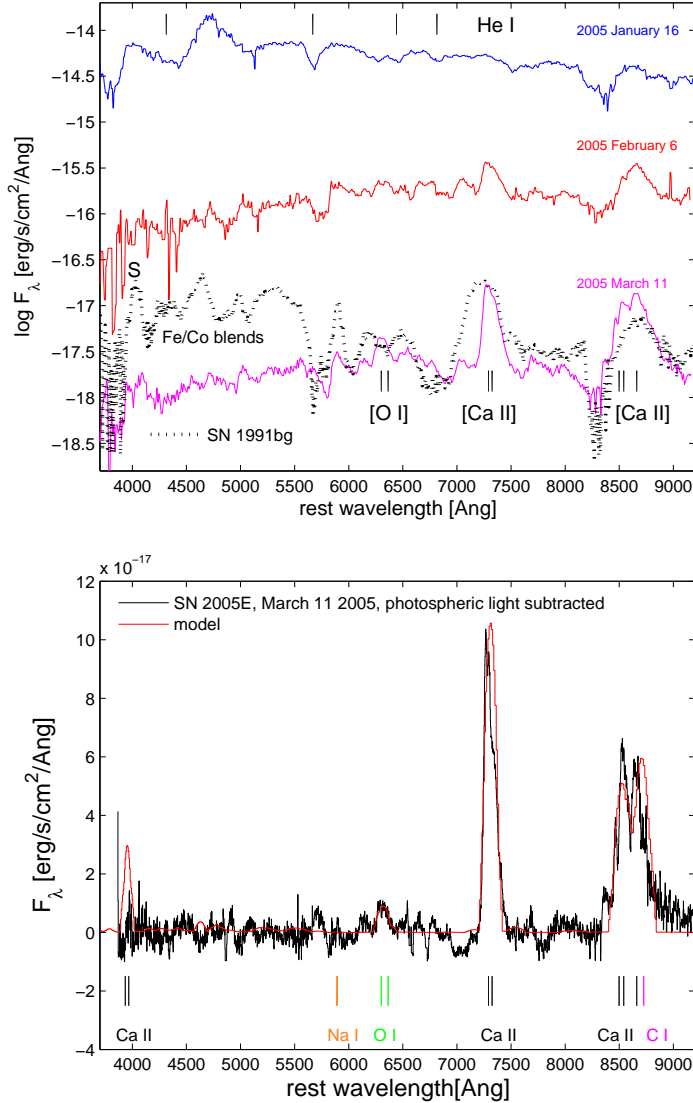


**Figure 2.** The mass and composition of the SN 2005E ejecta (technical details of observations can be found in SI Section 1). Upper panel: Photospheric spectra of SN 2005E. The top spectrum is obviously photospheric and shows absorption lines of the He I series (marked with black ticks after application of an  $11,000 \text{ km s}^{-1}$  blueshift, at the top). Nebular lines of intermediate-mass elements, most notably oxygen and calcium, begin to emerge in the middle spectrum, and dominate the latest nebular spectrum at the bottom. Also note that the typical Si lines of SNe Ia are absent in all spectra, while the nebular spectrum of SN 2005E clearly rules out a type Ia identification (comparison with the underluminous SN 1991bg<sup>11</sup> is shown; note the lack of the typical iron group line blends in the blue side). The derived line velocities are consistent with SN 2005E exploding within its putative host galaxy, NGC 1032. Bottom: The nebular spectrum of SN 2005E compared with a model fit. From the fit we can derive elemental abundances and masses in the ejecta of SN 2005E. We find masses of  $0.1$ ,  $0.02$ ,  $0.06$ ,  $0.003 M_{\odot}$  for carbon, oxygen, calcium, and radioactive nickel, respectively. Both the low total ejected mass of  $\sim 0.2 M_{\odot}$  and the relative abundances are unique among previously studied events.

assuming that some of the mass is not accounted for by the nebular spectrum analysis, e.g., high-velocity He layers and some slowly moving, denser ejecta that are still hidden below the photosphere at that time. Finally, SN 2005E shows a remarkable amount of calcium in its ejecta,  $0.06 M_{\odot}$  ( $\sim 0.22 \pm 0.08$  of the total ejecta mass), 5–10 times larger than any other type of SN<sup>5,6</sup> (25–350 times higher in relative calcium fraction).

The old environment, ejected mass, and nucleosynthetic output of SN 2005E are in stark contrast to those expected from collapsing massive stars, whether formed locally or ejected from a distant location (SI, Sections 5–6). The low ejected mass is also inconsistent with those determined for SNe Ia, restricted to a tight mass range of  $\sim 1\text{--}1.3 M_{\odot}$ , regardless of their intrinsic luminosity (even the prototype faint SN 1991bg is found in this range).<sup>4</sup> Furthermore, the light curve of SN 2005E (see SI, section 4) shows a different behavior than that of SNe Ia, declining much faster than even the most subluminous (1991bg like) SNe observed.<sup>3</sup> These properties, together with the observed spectra and our nucleosynthetic analysis, rules out SN 2005E as either a regular or peculiar SN Ia. Therefore, we conclude that SN 2005E is the first clearly identified example of a new, different type of SN explosion, arising from a low-mass progenitor.

The spectroscopic signatures of SN 2005E are quite unique, and allow one to identify additional similar events.<sup>7</sup> Arising from lower-mass progenitors, these events are likely to be found among both old and young stellar populations, i.e., we expect to find such peculiar SNe Ib in both early- and late-type galaxies. Indeed, while the unusual location of SN 2005E triggered the current study, several other calcium-rich subluminous SNe Ib/c similar to SN 2005E have been observed (see SI, Section 7). In addition, it is likely that other type Ib/c SNe observed in early type galaxies<sup>12,13</sup> could now be explained as originating from an old, low mass stellar population, and belonging to the family of Ca-rich SNe (see SI, Section 7). These SNe are therefore expected to show Ca-rich spectrum. Of the group of seven subluminous calcium-rich SNe Ib/c we identified, three are observed in old-population environments: SN 2005E presented here, as well as SN 2000ds and SN 2007ke, observed in elliptical galaxies. Moreover, SN 2000ds has pre- and post-explosion *Hubble Space Telescope* images showing no evidence for either star-forming regions or massive stars<sup>14</sup> near its location. No radio signature has been observed either.<sup>15</sup>

The rate of calcium-rich, faint, type Ib/c SNe can be estimated, since SN 2005E was discovered as part of the Lick Observatory Supernova Search (LOSS).<sup>10</sup> This survey is a volume-limited search, with high sensitivity within 60 Mpc for both SNe Ia and faint Ca-rich objects such as SN 2005E. LOSS found 2.3 calcium-rich objects (after correction

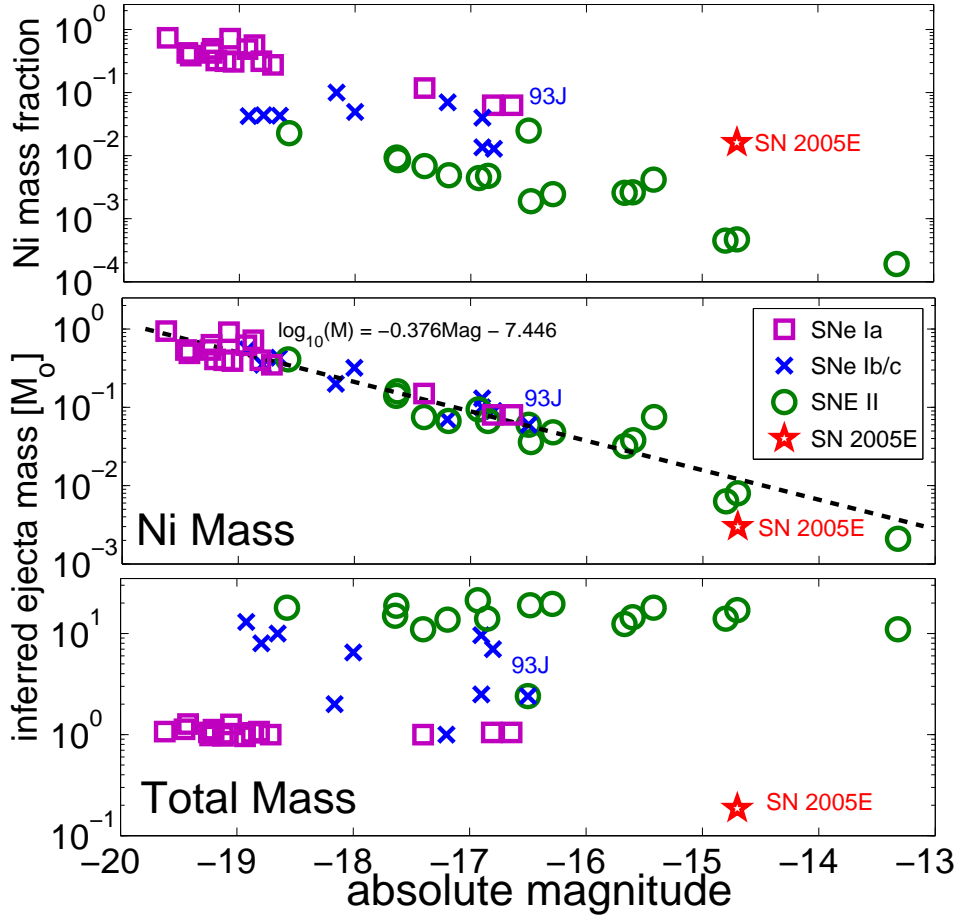


**Figure 3.** Comparison of the SN 2005E ejecta mass and luminosity with other SNe [SNe Ia, squares; SNe Ib/c,  $\times$  marks; SNe II, circles]. The lower panel shows the total ejecta mass inferred for SN 2005E, which is the lowest inferred ejecta mass found for any SN, based on nebular spectra. Its position in the luminosity vs. ejecta-mass phase space is unique, suggesting it is not a member of currently well-known SN families. The middle panel shows the Ni mass inferred for SN 2005E. The small Ni mass inferred for SN 2005E is consistent with its low luminosity, although somewhat lower than might be expected from the extension of the observed Ni mass-luminosity relation observed for other SNe (dashed line and formula). The upper panel shows the Ni ejecta mass fraction  $M_{\text{Ni}}/M_{\text{total}}$  inferred for SN 2005E. The sources from which the SN data were collected are listed in the SI, Section 8.

for incompleteness) and 31.0 SNe Ia in this volume, from which we infer the rate of such calcium-rich SNe to be  $7\% \pm 5\%$  of the total SN Ia rate. Further analysis of this group of subluminescent calcium-enriched SNe will be discussed in a forthcoming publication.

Given the unique nucleosynthetic products we observed, we ran several nucleosynthesis single-zone simulations<sup>16</sup> in order to investigate possible conditions that may lead to such signatures. We explored the ignition of various initial mixtures of He, C, and O on a grid of temperatures  $[(2-4) \times 10^9 \text{ K}]$ . We find that our essential results, namely, large calcium yield with little or no sulfur (in particular, the nebular analysis places a limit of calcium/sulfur  $> 6$ ), and a low mass of radioactive nickel and iron-group elements, can be robustly produced from initial compositions dominated by helium ( $X(\text{He}) \geq 0.5$ ; see SI, Section 9).

Calcium-rich SNe were theoretically predicted to arise from burning helium-rich material on a WD, leading to the full disruption of a sub-Chandrasekhar-mass WD.<sup>17,18</sup> However, such models predicted the production of SNe far more luminous (and  $^{56}\text{Fe}$  rich) than SN 2005E. Several theoretical models were suggested in the literature to possibly produce subluminescent SNe, with low-mass, high-velocity ejecta in an old stellar population. These include the accretion-induced collapse (AIC) of a WD (e.g. refs. 19 and 20), and the detonation of an accreted helium shell on a WD in a binary system (the “.Ia” model<sup>21,22</sup>). These studies did not explore the burning of large helium masses ( $> 0.1 M_{\odot}$ ), nor the production of calcium-rich ejecta. Multi-dimensional simulations of detonation in accreted He layers<sup>23</sup> showed (for their lowest mass white dwarfs;  $M = 0.7 M_{\odot}$ ) a trend toward high Ca/S and a light curve that was faster and dimmer than typical SNe Ia (but still much more luminous than SN 2005E), as well as a high production of  $^{44}\text{Ti}$ . It is possible that similar models, with less burning of C and O to make S and Ni, may resemble SN2005E better. Further studies in these directions are in progress.

We conclude that SN 2005E appears to be the first example identified where the theoretically suggested helium detonation process, and its unique nucleosynthetic production,<sup>17</sup> are observed. Additional characteristics of these explosions, including their old population origin, subluminescence, and low ejected mass, are broadly consistent with the predictions of some theoretical models (.Ia<sup>21</sup> and AIC<sup>20</sup>), variants of which may produce the appropriate conditions for such helium detonations. Alternatively, these explosions may require a totally new mechanism.

We note that the recently discovered peculiar subluminescent type Ia SN 2008ha<sup>24,25</sup> also shows prominent calcium-rich emission in its late-time spectrum. This may hint at the

involvement of a similar process of explosive helium burning in this peculiar object (see also SI, Section 10).

Our discovery has numerous astrophysical implications. It seems highly likely that we identified explosions arising from very close WD-WD systems, and therefore the rates of such events might be useful in constraining the rates of WD-WD inspirals observable as gravitational wave sources. The unique nucleosynthetic production of large masses of calcium and radioactive  $^{44}\text{Ti}$  per explosion could solve puzzles related to the source of calcium (especially  $^{44}\text{Ca}$ ) in the primitive solar system,<sup>26–28</sup> in old, metal-poor halo stars,<sup>29</sup> and the enrichment patterns of the interstellar and intracluster medium.<sup>30</sup> Production of most of the Galactic  $^{44}\text{Ti}$  and its progeny,  $^{44}\text{Ca}$ , in a few rare, prolific explosions, can also explain the origins of Galactic  $^{44}\text{Ca}$  given the null detection of  $^{44}\text{Ti}$  traces in most nearby SN remnants.<sup>28,31</sup>

Finally, products from inverse  $\beta$  decay of  $^{44}\text{Ti}$  may significantly contribute to the Galactic production of positrons.<sup>32</sup> Assuming our estimated rates ( $\sim 10\%$  of the SN Ia rate) and our  $^{44}\text{Ti}$  yield ( $0.006\text{--}0.06 M_{\odot}$ ; see SI, Section 9), Galactic SNe of the type we describe here will provide a significant contribution to the Galactic bulge component of the positron annihilation line, at least comparable to that of SNe Ia. In fact, within the current uncertainties on the  $^{44}\text{Ti}$  yield and SN rates, these events may come within a factor of few of producing all of the observed positrons.<sup>33</sup>

\*

## **Acknowledgements**

We would like to thank Udi Nakar and Dani Maoz for helpful comments. We acknowledge observations with the Liverpool Telescope, which is operated on the island of La Palma by Liverpool John Moores University in the Spanish Observatorio del Roque de los Muchachos of the Instituto de Astrofísica de Canarias with financial support from the UK Science and Technology Facilities Council. KAIT and its ongoing operation were made possible by donations from Sun Microsystems, Inc., the Hewlett-Packard Company, AutoScope Corporation, Lick Observatory, the NSF, the University of California, the Sylvia & Jim Katzman Foundation, and the TABASGO Foundation. Some of the data presented herein were obtained at the W. M. Keck Observatory, which is operated as a scientific partnership among the California Institute of Technology, the University of California, and NASA; the Observatory was made possible by the generous financial support of the W. M. Keck Foundation. We are grateful to the staffs of the Lick, Keck, and Palomar Observatories for their assistance. This research has made use of the NASA/IPAC Extragalactic Database (NED) which is operated by the Jet Propulsion Laboratory, California Institute of Technology, under contract with the National Aeronautics and Space Administration. A.G.-Y. acknowledges support by the Israeli Science Foundation, an EU Seventh Framework Programme Marie Curie IRG fellowship, the Benozziyo Center for Astrophysics, Minerva program, a research grant from the Peter and Patricia Gruber Awards, and the William Z. and Eda Bess Novick New Scientists Fund at the Weizmann Institute. A.V.F. is grateful for the support of US NSF grant AST-0607485, US Department of Energy grant DE-FG02-08ER41563, Gary and Cynthia Bengier, the Richard and Rhoda Goldman Fund, and the TABASGO Foundation.

\*Correspondence should be addressed to Avishay Gal-Yam (avishay.gal-yam@weizmann.ac.il) and Hagai Perets (hagai.perets@weizmann.ac.il).

## Supplementary Information

### (1) Technical observational details for figures 1 and 2

**Figure 1** Panel (a) shows the image of NGC 1032 prior to SN 2005E explosion, obtained from the SDSS. Panel (b) shows the LOSS<sup>10</sup> discovery of SN 2005E on Jan. 13, 2005. LOSS imaging of SN 2005E was obtained using the robotic 76-cm Katzman Automatic Imaging Telescope (KAIT) at Lick Observatory. Panel (c) shows an image of NGC 1032 in the light of the H $\alpha$  emission line, the panel shows the difference between images obtained using a narrow filter (6567 Å and a FWHM of 100Å) with a measured transmission of 40% for H alpha at the redshift of NGC 1032, plus broad R-band observations used for continuum subtraction. Exposure times of 1800 s, were obtained on Oct. 5, 2008 with the RATCam camera mounted on the 2-m Liverpool Telescope at Observatorio del Roque de Los Muchachos (La Palma, Spain). The smooth negative residual ( $\sim 7\%$  of the original flux) near the galaxy core probably arises from a combination of slight color gradients of the smooth galactic old population, and H $\alpha$  absorption in the spectra of old stars, and does not indicate real line emission. Panel (d) shows a zoom-in on the location of SN 2005E in pre-explosion SDSS  $r$ -band images. Panels (e)-(f) show deep photometry of the SN location using the Low-Resolution Imaging Spectrometer (LRIS)<sup>34</sup> mounted on the Keck-I 10-m telescope on Feb. 17, 2009 under very good conditions (seeing  $\sim 0.7''$ ). Panel (e) shows a red image with a total exposure time of 840 s, reaching a point-source detection limit of  $r < 25.3(25.9)$  mag at  $3(2)\sigma$ . Panel (f) shows a UV ( $u$ -band) image with a total exposure time of 780 s, reaching a point-source detection limit of  $u < 24.7(25.7)$  mag at  $3(2)\sigma$ . Panel (g) shows a zoom-in on the location of SN 2005E in H $\alpha$  light (same observations used to produce panel (c)).

**Figure 2** Upper panel: Photospheric spectra of SN 2005E. The top 2 spectra were obtained as part of the Caltech Core-Collapse Project (CCCP)<sup>35</sup> using the double spectrograph<sup>36</sup> mounted on the 5-m Hale telescope at Palomar Observatory. Exposure times were 600 s and 900 s on 2006 January 16 and February 6, respectively, with the 158 lines  $\text{mm}^{-1}$  and 1,200 lines  $\text{mm}^{-1}$  gratings, yielding an instrumental resolution of  $\sim 5$  Å and  $\sim 0.5$  Å on the red and blue sides, respectively. The CCCP spectra were further rebinned to  $\sim 5$  Å resolution bins to increase the signal-to-noise ratio. The bottom spectrum was obtained using LRIS<sup>34</sup> mounted on the Keck I 10-m telescope on 2005 March 11. We took an exposure of 600 s using the 560 dichroic and the 400/8500 grating and 600/4000

grism, giving resolutions of  $5.6 \text{ \AA}$  and  $2.4 \text{ \AA}$  in the red and blue sides, respectively. For comparison we plot a nebular spectrum of SN 1991bg; see Ref. 11 for a detailed discussion.

**(2) Can the progenitor of SN 2005E be a massive star formed in a star-forming region in the halo?**

Massive stars are typically formed and observed in giant molecular clouds and young stellar clusters or associations.<sup>37,38</sup> Core-collapse SNe of massive stars are therefore expected to be typically found close to star forming regions (SFRs). Observations of such SNe are usually consistent with this picture.<sup>39</sup> In principle, the discovery of SN 2005E in the halo of NGC 1032 could be attributed to in-situ star formation of a massive star rather than a low-mass older progenitor. However, star formation in the halo environment of a S0/a galaxy would be difficult to understand according to current star-formation theories. For example, star formation during collisions between cloudlets within high-velocity clouds at high galactic latitudes<sup>40</sup> has been shown to be much too rare.<sup>41</sup> Spiral density waves in the disk may trigger star formation up to a kpc above the Galactic plane,<sup>42</sup> but this seems unlikely for the larger height of SN 2005E (which also seems to be positioned beyond the edge of the optical disk). In addition, we note that NGC 1032 shows no evidence for warping or other structures extending beyond the region of the galactic disk to which SN 2005E could be related. We conclude that given the remote location of the supernova in the galactic halo, and the nondetection of any star-formation activity anywhere in the halo or the disk of NGC 1032, it is unlikely that an in-situ formation scenario could explain SN 2005E, unless a yet unknown and unique star-formation mechanism was at work in this case. In contrast, the evidence for a low-mass progenitor of SN 2005E is naturally consistent with the low-mass old stellar population environment in which it was found.

**A search for nearby star-forming regions:**

We have looked for star-formation tracers both in the halo and the disk of NGC 1032. Star-formation regions (SFRs) produce two classes of emission: continuum emission from young stars and emission lines (dominated by  $H\alpha$ ) produced by ionized gas. We have searched for both classes of emission, and obtained upper limits on the star-formation rates.

**$H\alpha$  observations:**

$H\alpha$  imaging was obtained with the Liverpool Telescope, and then analyzed using similar methods to those described in detail elsewhere.<sup>39</sup> We have determined an upper

limit of  $2.02 \times 10^{-17}$  erg cm $^{-2}$  for the H $\alpha$  flux from the region of SN 2005E. This is a  $3\sigma$  upper limit obtained from the variation in the sky background, for a  $2''$  aperture centered on the SN position and calibrated using an  $R$ -band galaxy magnitude taken from the literature.<sup>43</sup> For the distance of NGC 1032 (34 Mpc) we infer an H $\alpha$  luminosity of  $2.79 \times 10^{36}$  erg s $^{-1}$ ; correcting this for Galactic extinction (0.098 mag) and for the contribution from [N II] lines<sup>44</sup> we then calculate a corrected limit of  $H\alpha_{\text{limit}} = 2.3 \times 10^{36}$  erg s $^{-1}$ . Using the conversion rate from Ref. 9 (Eq. 2), we determine an upper limit on the star-formation rate at the SN position of  $SFR_{\text{limit}} = 1.8 \times 10^{-5}$  M $_{\odot}$  yr $^{-1}$ .

In addition, our H $\alpha$  observations of NGC 1032 show no SFRs closer than the galactic nucleus itself (see Fig. 1), up to our detection limit.

#### **$R$ - and $u'$ -band observations:**

Our deep  $R$  and  $u'$ -band observations using Keck (calibrated onto the SDSS photometric system) rule out point sources near the location of SN 2005E down to  $u' < 24.7$  (25.7),  $r < 25.3$  (25.9) mag at  $3(2)\sigma$  (see Fig. 1). At the distance of NGC 1032, these limits ( $M_r < -7.5$  ( $-6.9$ ) and  $M_{u'} < -8.1$  ( $-7.1$ ) mag at  $3(2)\sigma$ , respectively) indicate that we would have detected faint star-forming galaxies or star-forming regions at the SN location, or indeed even individual red supergiant or luminous blue supergiant stars. Since massive stars are usually formed and observed in stellar clusters or associations,<sup>37,38</sup> the lack of nearby supergiants (either red or blue) further argues against local star-formation activity.

#### **Radio signature of a core-collapse SN:**

A non-negligible fraction of core-collapse SNe show radio signatures. We have therefore made observations at 8.46 GHz with the VLA radio telescope on Jan. 21.10, 2005. We found a flux of  $11 \pm 53 \mu\text{Jy}$  at the optical position of SN 2005E. At the distance of SN 2005E, and assuming an explosion date between Dec. 24, 2004 and Jan. 14, 2005, the radio luminosity limit ( $2\sigma$ ) is  $1.8 \times 10^{26}$  erg s $^{-1}$  Hz $^{-1}$  which is a factor of 10 lower than a typical radio-emitting SNe Ib/c on this same timescale.<sup>45</sup>

#### **(3) Spectroscopic identification of SN 2005E as a type Ib supernova**

In Fig. 2 we show optical spectra of SN 2005E. Our first spectrum (Fig. 2 top, blue curve) is clearly photospheric, dominated by absorption lines including the He I series at  $\lambda\lambda 4471, 5876, 6678, 7065 \text{ \AA}$ , blueshifted by  $\sim 11,000$  km s $^{-1}$  (marked with black ticks at the top of Fig. 2), typical of a young SN Ib. Based on pre-discovery nondetections, SN 2005E was 3 – 20 days after explosion at this time. Analysis using the *Superfit* spectral

analysis code<sup>46</sup> confirms a type Ib identification, with the best-fit match being with a spectrum of the type Ib/c transition event SN 1999ex<sup>47</sup> 14 days after maximum light.

Our next spectrum (Fig. 2 middle, red curve) shows the beginning of the transition to the nebular phase, with emerging emission lines of oxygen and calcium. The best-fit spectrum found by *superfit* is that of the type Ic event SN 1990U, but spectra of the type Ib SN 1999di also provide a good fit. Masking of the blueshifted He I 6678 Å line by the emerging strong [O I]  $\lambda\lambda$ 6300, 6364 nebular doublet may account for the similarity to type Ic supernovae, with intrinsically much weaker He I lines.

Strong nebular emission lines of [O I]  $\lambda\lambda$ 6300, 6364 and [Ca II]  $\lambda\lambda$ 7291, 7324 and the near-infrared triplet at  $\lambda\lambda$ 8498, 8542, 8662 (tick marks at the bottom of Fig. 2) dominate our latest spectrum of SN 2005E (Fig. 2 bottom, magenta curve). The best fit found by *Superfit* is to the type Ib SN 1985F<sup>48,49</sup> obtained 89 days after its first observation. Dominated by lines of intermediate-mass elements (O and Ca), the nebular spectrum of SN2005E is similar to that of type Ib events, though calcium is much stronger than usual for these SNe type, while the lack of Fe-group emission lines in the bluer part of the spectrum rules out an identification as a type Ia event of either the normal or subluminous (SN 1991bg like<sup>2</sup>) varieties.

#### (4) Ejected mass estimates from the observed light curve and photospheric velocities:

The ejecta mass of a given supernova can be estimated using its light curve and the observed ejecta velocities. The ejecta velocity of a SN is proportional to  $(E_{\text{kin}}/M_{\text{ej}})^{1/2}$ , where  $E_{\text{kin}}$  is the kinetic energy and the  $M_{\text{ej}}$  is the ejecta mass, while the typical duration of a SN light curve is  $t_{\text{d}} \propto (M_{\text{ej}}^3/E_{\text{kin}})^{1/4}$ .<sup>50</sup> Combining these equations and assuming that two objects have the same opacity, we have

$$E_{\text{kin},1}/E_{\text{kin},2} = \left(\frac{v_1}{v_2}\right)^3 \left(\frac{t_1}{t_2}\right)^2 \quad (1)$$

and

$$M_{\text{ej},1}/M_{\text{ej},2} = \frac{v_1}{v_2} \left(\frac{t_1}{t_2}\right)^2. \quad (2)$$

Following Ref. 24 who estimated the mass of the subluminous SN 2008ha, we use a normal SN Ia as a reference with  $t_{\text{d}} = 19.5$  days and  $v = 8,000$  km s<sup>-1</sup>.<sup>51</sup> The timescales of SN 2005E are 0.4 – 0.5 times shorter than those of the well-observed type Ib SN 2008D (the stretched light curve of SN 2008D is shown in Fig. S1 for comparison), which had a rise time of 18 days,<sup>52</sup> and therefore we estimate the rise time of SN 2005E to be 7 – 9

days. The ejecta velocities we observe from the photospheric spectra are  $11,000 \text{ km s}^{-1}$ . We therefore find  $E_{\text{kin},05e}/E_{\text{kin,Ia}} = 0.34\text{--}0.55$  and  $M_{\text{ej},05e}/M_{\text{ej,Ia}} = 0.17 - 0.29$ . Assuming  $E_{\text{kin,Ia}} = 1.3 \times 10^{51}$  ergs and  $M_{\text{ej,Ia}} = 1.4 M_{\odot}$ , we find  $E_{\text{kin},05e} = (4.4 - 7.2) \times 10^{50}$  ergs and  $M_{\text{ej},05e} = 0.25 - 0.41 M_{\odot}$ . We note that this widely used method for SN ejecta-mass estimation may have two caveats in our case: helium is less opaque than other elements so we may miss some of the helium mass, and  $^{56}\text{Ni}$  may not be the only radioactive energy source as assumed in such estimates.

**(5) The possible origin of SN 2005E from a hypervelocity star and its trajectory:**

Most of the stars in the Galaxy move at relatively low velocities (a few tens of  $\text{km s}^{-1}$ ) with respect to their Galactic environment. Some massive stars ( $\gtrsim 8 M_{\odot}$ ) are known to have higher velocities, up to  $\sim 200 \text{ km s}^{-1}$ . These so-called “runaway stars” are ejected from their birth place as a result of binary encounters, or if they have binary companions that explode as SNe,<sup>55,56</sup> and could therefore be found far from the SFR where they were formed. Hypervelocity stars<sup>57</sup> (HVSs) move at even higher velocities ( $\text{few} \times 10^2\text{--}10^3 \text{ km s}^{-1}$ ). Such stars are thought to be ejected following dynamical interaction with (or close to) massive black holes.

In 2005, the first HVS was serendipitously discovered in the Galactic halo,<sup>58</sup> 71 kpc from the Galactic center, with a radial velocity of  $853 \pm 12 \text{ km s}^{-1}$ . Two additional HVSs, one of them a massive B star with  $\sim 9 M_{\odot}$ , were discovered shortly thereafter.<sup>59,60</sup> Follow-up surveys have discovered a total of  $\sim 20$  HVSs with radial velocities in the range  $300\text{--}900 \text{ km s}^{-1}$  at distances of  $20\text{--}120$  kpc from the Galactic center (GC). A total population of  $\sim 100$  such young B stars is inferred to exist in the Galaxy at these distances (no main-sequence O stars are observed). Given their positions and velocities, all observed HVSs must have been ejected with even higher initial velocities ( $> 850 \text{ km s}^{-1}$ ), if they originated near the massive black hole (MBH) in the center of our Galaxy whose mass is  $\sim 3.6 \times 10^6 M_{\odot}$ .<sup>61,62</sup>

If the progenitor of SN 2005E was a massive star, it could have formed in the center or the disk of NGC 1032 and then have been ejected at high velocity to attain its observed location in the halo. In order to find the ejection velocity required for the progenitor of SN 2005E to travel from its birth place to the observed position of SN 2005E, we need to trace its possible trajectory. For this purpose we need to assume some galactic potential for NGC 1032 to be used for the calculations of the HVS trajectory. For the galactic potential we use a two-component model suggested in Ref. 63 composed of a galactic bulge, and

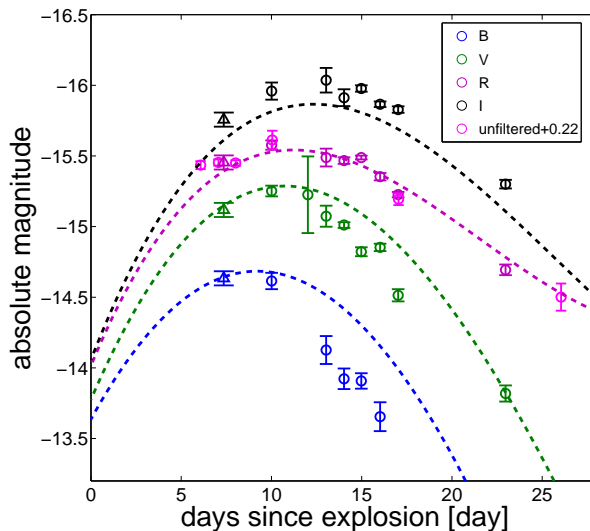


**Figure 4.** Optical light curves of SN 2005E. Top: We present our observations obtained using the 0.76-m KAIT as part of LOSS<sup>10</sup> in the *BVRI* bands (blue, green, red, and black empty circles, respectively), as well as unfiltered data (magenta empty circles). Additional point (triangle) was obtained through synthesis of the first spectrum (seen in Fig. 1), scaled to fit the *R*-band photometry. KAIT unfiltered observations are most similar to *R*-band data due to the combined response of its optics and detector, so we have scaled these data to the *R*-band observations. The rapid decline of this object is consistent<sup>53</sup> with its relatively low absolute magnitude,  $M_R \approx -15.5$ , calculated assuming a distance of 34 Mpc to NGC 1032 (as given in the NED database<sup>54</sup>) and negligible extinction. Estimating the peak date of this SN from the magenta curve (January 7, 2005), our spectra (Fig. 2) were obtained 9, 29, and 62 days after maximum light. The rapid decline observed in the light curve is similar to that of observed subluminous SNe Ia at early times, with a slope of  $-0.155 \text{ mag day}^{-1}$ , but it does not show a break to a different slope expected at  $\sim 4.5$  days after peak (compare with the analysis of Kasliwal et al.<sup>3</sup>). Also shown for comparison are third order polynomial fits to the light curves of the well-studied type Ib SN 2008D.<sup>52</sup> We find that SN 2005E behaves similarly to SN 2008D, but with timescales roughly a factor of 0.45–0.55 shorter (the displayed light curves of SN 2008D are stretched by a factor of 0.52).

a halo (the disk component has a relatively small effect). Ref. 8 finds the virial mass of galaxies such as NGC 1032 to be  $\sim 1.5 \times 10^{12} M_{\odot}$  for magnitudes  $-19.5 < M_B < -20.5$  where NGC 1032 has  $M_B = -19.8$  mag. This mass is also generally consistent with the formulas in Ref. 64, which gives a total galactic mass of  $(2-3) \times 10^{12} M_{\odot}$  from the relation found for the MBH mass and the halo mass. The bulge mass could be estimated from the velocity dispersion in the bulge<sup>65</sup> to be between  $6 \times 10^{10} M_{\odot}$  and  $1.3 \times 10^{11} M_{\odot}$ , where the bulge size is  $\sim 1.85$  kpc.<sup>65</sup>

The inferred ejection velocity of the progenitor of SN 2005E from a birth place in the disk (taking the shortest distance from the observed position of SN 2005E to the plane of the galactic disk) is found to be  $> 1600 \text{ km s}^{-1}$  for a massive ( $\sim 25 M_{\odot}$ ), short-lived ( $\sim 7 \times 10^6$  yr) progenitor, appropriate for a type Ib SN. Such an ejection velocity from the galactic disk would require an ejection mechanism different from that of OB runaways, where the only suggested mechanisms involve an interaction with a MBH. Such a MBH is unlikely to exist in the galactic disk. An ejection velocity of  $> 300 \text{ km s}^{-1}$  would be required for a lower mass ( $\sim 8 M_{\odot}$ ) and longer lived ( $\sim 4 \times 10^7$  yr) component in a binary progenitor ejected from the disk. Such a velocity is much higher than the typical velocities of OB runaway stars,<sup>56</sup> but it could theoretically be accessible for a runaway single star.<sup>66</sup> However, runaway binaries are typically ejected at lower velocities (up to 0.3 – 0.4 of the maximal ejection velocities of single stars<sup>67</sup>), which would again suggest a different ejection mechanism than OB runaways. We conclude that the progenitor of SN 2005E is unlikely to be ejected from the disk by currently suggested high-velocity ejection mechanisms, and (if ejected at all) was more likely to be ejected from the center of NGC 1032.

For the progenitor of SN 2005E to be ejected from the galactic center and reach its current position in the halo during its lifetime, the required ejection velocity would be at least  $\sim 3400 \text{ km s}^{-1}$  ( $\sim 1600 \text{ km s}^{-1}$ ) assuming a lifetime of  $< 7$  Myr for a  $25 M_{\odot}$  star ( $< 40$  Myr for an  $8 M_{\odot}$  binary star). We now calculate whether such ejection velocities are likely, taking into account the conditions in NGC 1032.

Given the velocity dispersion in the bulge of NGC 1032, which is in the range<sup>65</sup> 200–225  $\text{km s}^{-1}$ , we can estimate the mass of the MBH in the nucleus using the  $M - \sigma$  relation<sup>68,69</sup> to be in the range  $\sim (1-2) \times 10^8 M_{\odot}$ .

We now compare the velocities derived from the trajectories with the average ejection velocity of a star ejected from the galactic nucleus following the disruption of a binary by

a MBH, given by<sup>70,71</sup>

$$v_{\text{eject}} = 3400 \text{ km s}^{-1} \times \left( \frac{a_{\text{bin}}}{0.8 \text{ AU}} \right)^{-1/2} \left( \frac{M_{\text{bin}}}{50 M_{\odot}} \right)^{1/3} \left( \frac{M_{\text{BH}}}{1.5 \times 10^8 M_{\odot}} \right)^{1/6},$$

where  $a_{\text{bin}}$  is the semi-major axis of the binary,  $M_{\text{bin}}$  is the binary mass, and  $M_{\text{BH}}$  is the MBH mass. Massive binaries usually have components of comparable and frequently equal mass, and are known to have relatively compact orbits, with a large fraction of them ( $f_{\text{cbin}} \approx 0.4$ ) in close binaries ( $a_{\text{bin}} < 1 \text{ AU}$ ; e.g., Refs. 72,73 and 74). We therefore conclude that the observed position of SN 2005E is consistent with its progenitor being ejected as a massive star following the disruption of a typical very massive binary of  $M_{\text{bin}} = 2 \times 25 = 50 M_{\odot}$  and  $a_{\text{bin}} \lesssim 0.8 \text{ AU}$ , or the disruption of a  $M_{\text{triple}} = 3 \times 8 = 24 M_{\odot}$  triple star, with an outer semi-major axis of  $a_{\text{bin}} \lesssim 1.5 \text{ AU}$ , which would eject a hypervelocity binary.<sup>75</sup>

The velocity of an observed supernova is difficult to measure. The measured velocities of the supernova ejecta are on the order of a few thousands  $\text{km s}^{-1}$  and any signature of a pre-explosion velocity of the progenitor is smeared out even for velocities as high as hundreds of  $\text{km s}^{-1}$ . Even for higher velocities such as expected for a HVS, one would require extreme velocities for the HVS, directed along the line of sight, in order to identify a significant signature of the SN HVS progenitor. The velocities we find for SN 2005E ejecta velocities are consistent with other SN Ib/c ejecta velocities at the various epochs.

### (6) The ejection rate of hypervelocity stars:

Although two massive HVS ( $> 8 M_{\odot}$ ; Refs. 59 and 76) are known in our Galaxy, it is difficult to infer the total number of Galactic massive HVSs from the very few examples known, given their serendipitous discovery nature. An estimate can be obtained if most massive HVSs in our Galaxy have been ejected through the Hills binary disruption mechanism<sup>57,77</sup> (which is the likely case<sup>78–80</sup>). In this scenario the binary companions of ejected HVSs should have been captured into close orbits around the MBH<sup>81,77</sup>; the number of such stars should therefore reflect the number of similar HVSs in the Galaxy. Currently, a few tens of main-sequence B stars are observed in such close orbits ( $< 0.04 \text{ pc}$  from the MBH; e.g. Ref. 82). Approximately half of these stars (with identified stellar types) are found to be B0-2 V main sequence stars, most likely with masses  $> 8 M_{\odot}$ . Given the trend of massive binaries to have equal-mass components,<sup>72</sup> one can then infer a total of  $\sim 10$ – $20$  such massive HVSs in our Galaxy. The total number of  $> 8 M_{\odot}$  stars in the Galaxy is  $\sim 10^6$  stars (e.g., assuming a Miller-Scalo initial mass function); thus, the HVS fraction of the population of massive stars is  $\sim 10/10^6 = 10^{-5}$ , and we therefore

SN	Absolute $B$ -band peak magnitude	Absolute $B$ -band discovery magnitude	Host galaxy	Host-galaxy type
2000ds	?	-13.32*	NGC 2768	E/S0
2001co	-15.09*	-14.77*	NGC 5559	Sb
2003H	?	-13.43*	NGC 2207	Galaxy pair
2003dg	?	-15.03*	UGC 6934	Scd
2003dr	-14.04*	-13.8*	NGC 5714	Sc
2005E	-14.8	-14.7	NGC 1132	S0/Sa
2007ke	-15.45*	-14.7*	NGC 1129	E/S0

**Table 1.** The sample of calcium-rich SNe

Discovery of these SNe is reported in Refs. 83 (2000ds), 84 (2001co), 85 (2003H), 86 (2003dg), 87 (2003dr), 88 (2005E) and 89 (2007ke).

\* $B$  magnitude unavailable; unfiltered used, corrected to  $B$  using the measured colors of SN 2005E at peak.

expect a similar fraction of HVS supernova progenitors. If the progenitor of SN 2005E was a hypervelocity star, the probability of discovering SN 2005E in LOSS, which detected a total of  $\sim 550$  core-collapse SNe from 1998 through 2008, is low. Its discovery would then be either a chance observation of a rare event, or suggests a much higher ejection rate of extragalactic HVSs than observed in our Galaxy. However, given the low-mass ejecta observed for SN 2005E and its additional peculiarities, which cannot be explained by a hypervelocity progenitor, it is more likely that SN 2005E has a different origin.

### (7) Additional calcium-rich faint type Ib/c SNe:

In addition to SN 2005E, several other objects were reported as possible members of this class of calcium-rich SNe. We have verified these reports by re-inspection of the spectra, rejecting unconvincing cases, and list all verified Ca-rich events in Table 1.

A full analysis of the photometry and spectroscopy of this extended sample will be presented in a forthcoming publication.

In addition, other type Ib/c SNe observed in early type (elliptical or S0) galaxies<sup>12,13</sup> could possibly be explained as originating from an old, low mass stellar population, and belonging to our family of Ca-rich SNe. These include<sup>13</sup> SNe 2000ds, 2002jj, 2002hz, 2003ih, 2005cz and 2006ab. Of these we confirmed SN 2000ds to be a Ca-rich SN (it was independently classified as such; see table 1). Early spectra of SNe 2003ih and 2006ab suggest that these SNe are not Ca-rich SNe, however, later spectra than available to us are required in order to exclude this with better confidence. We have not yet confirmed nor excluded the Ca-rich classification of the other candidates in the list. Note, however, that

the host galaxies of SNe 2002jj, 2002hz, 2003ih and 2006ab were re-classified in Ref. 13 to be late type galaxies, leaving only SNe 2000ds (Ca-rich confirmed) and 2005cz (candidate) as type Ib/c in early type galaxies, where the host galaxy of the latter is suspected to have been involved in a merger event<sup>90</sup> and possibly fairly recent star formation as well.<sup>91</sup>

**(8) Masses and luminosities of SNe:**

In Fig. 3 we compared the nickel mass and the total mass and luminosity of SN 2005E with those of other SNe. The data used in this figure were taken from the literature, as follows. The data for SNe Ia were taken from Ref. 4 and references therein; it includes both typical SNe as well as peculiar and subluminous SNe. The data for SNe Ib/c were collected from Refs. 92, 93, 94, 95, and 96. Additional data concerning the ejected Ni mass were taken from Ref. 97. The data for SNe II were taken from Refs. 98 and 99, and contain both regular and subluminous SNe, most of them SNe IIP.

**(9) Nucleosynthetic simulations:**

We ran several single-zone simulations using the JINA version of ReaLib (April 2009) for the rates, a 203-nucleus network, and the “explosive nucleosynthesis” procedure.<sup>16</sup> We investigated various initial compositions of He, C, and O, at a density of  $10^6 \text{ g cm}^{-3}$ , and scanned the temperature range  $(2\text{--}4.1) \times 10^9 \text{ K}$ . Our main findings are illustrated in Fig. S2 and Table 2. In Fig. S2, we scale the mass fractions to fit the observed calcium abundance, and plot the observed limits on sulfur and  $^{56}\text{Ni}$ . We also present the amount of  $^{44}\text{Ti}$  produced. A 0.6/0.4 mix of He/O **(a)** works well in reproducing our data only up to  $T_9 = 3.5$  where nickel becomes overabundant, and certainly fails at higher  $T$ , where S is also a problem. In the allowed phase space ( $T_9 < 3.5$ ),  $^{44}\text{Ti}$  is 0.1–0.3 times as abundant as Ca. Increasing the amount of helium **(b)**, only low temperatures ( $T_9 = 2.2$ ) are allowed; in this case radioactive titanium and calcium are almost equally produced. Replacing oxygen by pure carbon **(c)** does not work for nearly equal ratios, as we either get too much S or too much Ni, or both. Decreasing the amount of carbon **(d)** again works only for the lowest temperatures,  $T_9 = 2.2$ , leading to significant production of  $^{44}\text{Ti}$ .

We conclude that helium-rich models with some C/O contamination can recover our essential findings. A prediction is that a substantial amount of  $^{44}\text{Ti}$  (at least 1/10 of Ca, and perhaps a comparable amount) will be synthesized. In some cases  $^{48}\text{Cr}$  production exceeds that of  $^{56}\text{Ni}$ ; its decay may therefore power the light curve (via  $^{48}\text{V}$  decay). A realistic model in which the burning shock traverses layers of varying temperature, density, and composition will be investigated in a forthcoming publication.

**(10) The origin of SN 2008ha-like SNe:**

We note that the low luminosity and calcium-rich late-time spectra of the recently discovered SN 2008ha<sup>24,25</sup> (see Fig. 7 of Ref. 24), may relate it to our group of calcium-rich faint SNe. Its type Ia identification suggests that its composition contains a larger fraction of C/O burning products than observed for SN 2005E. The first models suggesting the production of calcium-rich SNe through helium detonations<sup>17,18</sup> showed that helium burning on C/O WDs could produce calcium-rich SNe with various ejecta masses and luminosities, depending on the specific initial conditions used, and could sometimes lead to a C/O deflagration of the accreting WD. One could therefore expect a range of outcomes with varying mixtures of helium (Ca, Ti) and C/O burning (S, Si, Fe, Ni) products. This could be consistent with the wide variety of luminosities (and likely ejecta masses) found in other SNe similar to SN 2008ha,<sup>100,101,24,25</sup> including the helium-rich SN 2007J. If the possibility raised here is correct, we expect events of this distinct class of SNe (so-called

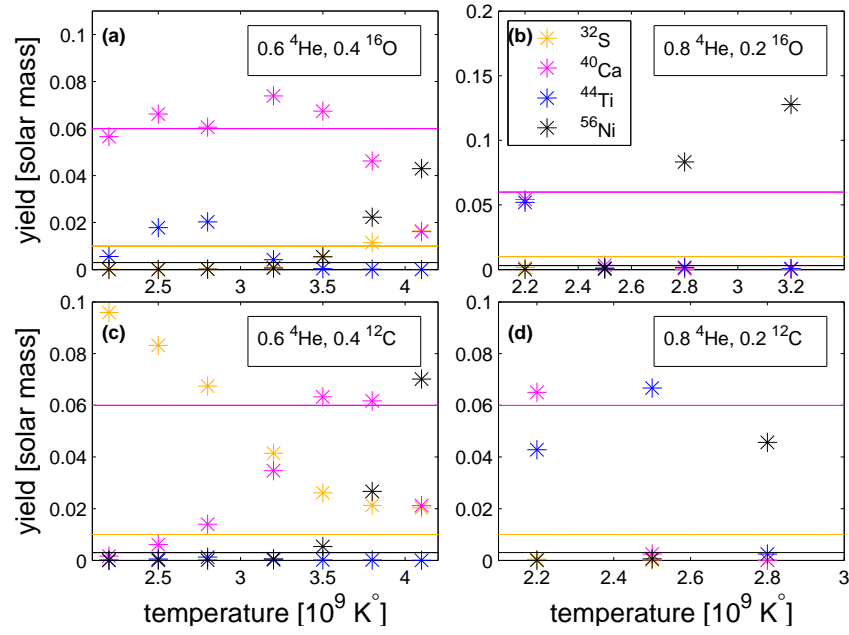


**Figure 5.** Nucleosynthetic products of the burning of He-rich mixtures with carbon and oxygen (fractions marked in each panel), at various temperatures and an initial density of  $10^6$  g  $\text{cm}^{-3}$ . The fractions are scaled to best match the observed calcium mass (cyan horizontal line) and compared with the observed limit on sulfur (ocher line) and measurement of radioactive  $^{56}\text{Ni}$  (black line).

Initial Conditions			Final Values					
$T_9$	${}^4\text{He}$	${}^{12}\text{C}$	${}^{32}\text{S}$	${}^{40}\text{Ca}$	${}^{44}\text{Ti}$	${}^{48}\text{Cr}$	${}^{52}\text{Fe}$	${}^{56}\text{Ni}$
3.4	$8.00 \times 10^{-1}$	$1.86 \times 10^{-1}$	$6.18 \times 10^{-5}$	$1.97 \times 10^{-4}$	$2.68 \times 10^{-4}$	$1.34 \times 10^{-4}$	$2.82 \times 10^{-4}$	$8.08 \times 10^{-1}$
3.4	$7.50 \times 10^{-1}$	$2.36 \times 10^{-1}$	$2.80 \times 10^{-4}$	$1.30 \times 10^{-1}$	$5.03 \times 10^{-3}$	$9.03 \times 10^{-3}$	$2.29 \times 10^{-1}$	$5.82 \times 10^{-1}$
3.4	$7.00 \times 10^{-1}$	$2.86 \times 10^{-1}$	$2.49 \times 10^{-3}$	$6.10 \times 10^{-1}$	$1.60 \times 10^{-1}$	$3.04 \times 10^{-2}$	$1.65 \times 10^{-1}$	$1.18 \times 10^{-1}$
3.4	$6.50 \times 10^{-1}$	$3.36 \times 10^{-1}$	$1.12 \times 10^{-1}$	$5.61 \times 10^{-1}$	$2.63 \times 10^{-3}$	$1.84 \times 10^{-2}$	$2.00 \times 10^{-2}$	$2.78 \times 10^{-2}$
3.4	$6.00 \times 10^{-1}$	$3.86 \times 10^{-1}$	$2.09 \times 10^{-1}$	$3.74 \times 10^{-1}$	$1.13 \times 10^{-3}$	$9.84 \times 10^{-3}$	$8.01 \times 10^{-3}$	$1.97 \times 10^{-2}$
3.2	$8.00 \times 10^{-1}$	$1.86 \times 10^{-1}$	$5.25 \times 10^{-5}$	$1.74 \times 10^{-4}$	$2.36 \times 10^{-4}$	$1.18 \times 10^{-4}$	$3.15 \times 10^{-4}$	$8.29 \times 10^{-1}$
3.2	$7.50 \times 10^{-1}$	$2.36 \times 10^{-1}$	$1.69 \times 10^{-6}$	$1.24 \times 10^{-1}$	$3.94 \times 10^{-1}$	$6.66 \times 10^{-2}$	$4.33 \times 10^{-1}$	$2.50 \times 10^{-1}$
3.2	$7.00 \times 10^{-1}$	$2.86 \times 10^{-1}$	$4.32 \times 10^{-4}$	$6.55 \times 10^{-1}$	$1.14 \times 10^{-1}$	$8.00 \times 10^{-2}$	$7.49 \times 10^{-2}$	$1.95 \times 10^{-2}$
3.2	$6.80 \times 10^{-1}$	$2.86 \times 10^{-1}$	$2.73 \times 10^{-2}$	$6.76 \times 10^{-1}$	$2.43 \times 10^{-2}$	$2.79 \times 10^{-2}$	$1.37 \times 10^{-2}$	$9.83 \times 10^{-3}$
3.2	$6.50 \times 10^{-1}$	$3.36 \times 10^{-1}$	$1.63 \times 10^{-1}$	$4.18 \times 10^{-1}$	$4.75 \times 10^{-3}$	$1.07 \times 10^{-2}$	$4.35 \times 10^{-3}$	$6.86 \times 10^{-3}$
3.2	$6.00 \times 10^{-1}$	$3.86 \times 10^{-1}$	$2.90 \times 10^{-1}$	$2.43 \times 10^{-1}$	$1.56 \times 10^{-3}$	$5.29 \times 10^{-3}$	$1.95 \times 10^{-3}$	$4.02 \times 10^{-3}$
3.0	$8.00 \times 10^{-1}$	$1.86 \times 10^{-1}$	$6.06 \times 10^{-5}$	$2.15 \times 10^{-4}$	$3.26 \times 10^{-4}$	$2.38 \times 10^{-4}$	$8.69 \times 10^{-2}$	$7.50 \times 10^{-1}$
3.0	$7.50 \times 10^{-1}$	$2.36 \times 10^{-1}$	$3.85 \times 10^{-9}$	$2.96 \times 10^{-2}$	$1.73 \times 10^{-1}$	$1.78 \times 10^{-1}$	$4.53 \times 10^{-1}$	$1.24 \times 10^{-1}$
3.0	$7.00 \times 10^{-1}$	$2.86 \times 10^{-1}$	$1.06 \times 10^{-3}$	$5.72 \times 10^{-1}$	$2.71 \times 10^{-1}$	$4.41 \times 10^{-2}$	$9.32 \times 10^{-3}$	$4.16 \times 10^{-3}$
3.0	$6.50 \times 10^{-1}$	$3.36 \times 10^{-1}$	$2.40 \times 10^{-1}$	$2.88 \times 10^{-1}$	$2.91 \times 10^{-2}$	$3.77 \times 10^{-3}$	$7.91 \times 10^{-4}$	$2.34 \times 10^{-3}$
3.0	$6.00 \times 10^{-1}$	$3.86 \times 10^{-1}$	$3.85 \times 10^{-1}$	$1.53 \times 10^{-1}$	$1.14 \times 10^{-1}$	$1.51 \times 10^{-3}$	$2.47 \times 10^{-4}$	$1.44 \times 10^{-3}$

**Table 2.** The abundances (by mass) of several important nuclei from post-shock burning in a helium-burning layer. A 203-nucleus network was used, with reaction rates taken from an April 2009 download of ReaLib from JINA. The initial composition was  ${}^4\text{He}$ ,  ${}^{12}\text{C}$  (see table for initial values; temperature  $T_9$  given in  $10^9$  K), and 0.014 of  ${}^{22}\text{Ne}$  by mass. The values of  ${}^4\text{He}$  and  ${}^{12}\text{C}$  correspond to different degrees of hydrostatic helium burning prior to explosion. Low values for S/Ca occur only for high  ${}^4\text{He}$  abundance. For such low S/Ca, temperature must be  $T < 3.2 \times 10^9$  K to avoid overproduction of  ${}^{56}\text{Ni}$ . Production of  ${}^{48}\text{Cr}$  (and  ${}^{52}\text{Fe}$ ) may exceed that of  ${}^{56}\text{Ni}$ , so that  ${}^{48}\text{V}$  decay (half-life 15.98 days) may help power the light curve.<sup>21</sup>  ${}^{44}\text{Ti}$  can be copiously produced under these conditions, so that such events may provide a solution to the problem of low emission from  ${}^{44}\text{Ti}$  decay. The significant abundance of  ${}^{12}\text{C}$  prior to the explosive burning may allow unburned (lower density) regions to explain the relatively large abundance of  ${}^{12}\text{C}$  observed. To convert the abundance entries to solar mass units, multiply by the assumed mass of ejecta.

SN 2002cx-like SNe<sup>100,101</sup>) to show a calcium-enhanced composition. Such a prediction could be checked in the future through spectral analysis of these SNe.

- 
1. Filippenko, A. V. Optical spectra of supernovae. *ARAA* **35**, 309–355 (1997).
  2. Filippenko, A. V. *et al.* The subluminous, spectroscopically peculiar type Ia supernova 1991bg in the elliptical galaxy NGC 4374. *AJ* **104**, 1543–1556 (1992).
  3. Kasliwal, M. M. *et al.* SN 2007ax: An extremely faint type Ia supernova. *ApJL* **683**, L29–L32 (2008).
  4. Mazzali, P. A. *et al.* A common explosion mechanism for type Ia supernovae. *Science* **315**, 825– (2007).
  5. Nomoto, K. *et al.* Nucleosynthesis in type Ia supernovae. *Nuclear Physics A* **621**, 467–476 (1997).
  6. Nomoto, K. *et al.* Nucleosynthesis in type II supernovae. *Nuclear Physics A* **616**, 79–90 (1997).
  7. Filippenko, A. V. *et al.* Supernovae 2001co, 2003H, 2003dg, and 2003dr. *IAU Circular* **8159**, 2–+ (2003).
  8. Prada, F. *et al.* Observing the dark matter density profile of isolated galaxies. *ApJ* **598**, 260–271 (2003).
  9. Kennicutt, Jr., R. C. Star formation in galaxies along the Hubble sequence. *ARA&A* **36**, 189–232 (1998).
  10. Filippenko, A. V. *et al.* in *IAU Colloq. 183: Small Telescope Astronomy on Global Scales* (eds Paczynski, B., Chen, W.-P. & Lemme, C.) 121–+ (ASP, 2001).
  11. Mazzali, P. A. *et al.* The properties of the peculiar type IA supernova 1991bg - II. The amount of <sup>56</sup>Ni and the total ejecta mass determined from spectrum synthesis and energetics considerations. *MNRAS* **284**, 151–171 (1997).
  12. van den Bergh, S., Li, W. & Filippenko, A. V. Classifications of the Host Galaxies of Supernovae, Set III. *PASP* **117**, 773–782 (2005).
  13. Hakobyan, A. A., Petrosian, A. R., McLean, B., Kunth, D., Allen, R. J. *et al.* Early-type galaxies with core collapse supernovae. *A&A* **488**, 523–531 (2008).
  14. Maund, J. R. & Smartt, S. J. Hubble Space Telescope imaging of the progenitor sites of six nearby core-collapse supernovae. *MNRAS* **360**, 288–304 (2005).

15. Soderberg, A. M. *et al.* Late-time radio observations of 68 type Ibc supernovae: Strong constraints on off-axis gamma-ray bursts. *ApJ* **638**, 930–937 (2006).
16. Arnett, D. *Supernovae and Nucleosynthesis. An Investigation of The History of Matter, from The Big Bang to The Present.* Princeton series in astrophysics, Princeton, NJ: Princeton University Press (1996).
17. Woosley, S. E., Taam, R. E. & Weaver, T. A. Models for type I supernova. I - Detonations in white dwarfs. *ApJ* **301**, 601–623 (1986).
18. Woosley, S. E. & Weaver, T. A. Sub-Chandrasekhar mass models for type Ia supernovae. *ApJ* **423**, 371–379 (1994).
19. Nomoto, K. & Kondo, Y. Conditions for accretion-induced collapse of white dwarfs. *ApJL* **367**, L19–L22 (1991).
20. Metzger, B. D., Piro, A. L. & Quataert, E. Nickel-rich outflows from accretion disks formed by the accretion-induced collapse of white dwarfs. *ArXiv* **0812.3656**, (2008).
21. Bildsten, L. *et al.* Faint thermonuclear supernovae from AM Canum Venaticorum binaries. *ApJL* **662**, L95–L98 (2007).
22. Shen, K. J. & Bildsten, L. Unstable helium shell burning on accreting white dwarfs. *ArXiv* **0903.0654**, (2009).
23. Livne, E. & Arnett, D. Explosions of sub-Chandrasekhar mass white dwarfs in two dimensions. *ApJ* **452**, 62+ (1995).
24. Foley, R. J. *et al.* SN 2008ha: An extremely low luminosity and extremely low energy supernova. *ArXiv* **0902.2794**, (2009).
25. Valenti, S. *et al.* An extremely faint stripped-envelope core-collapse supernova and its implications. *Nature, in press* **arXiv:0901.2074**, (2009).
26. Woosley, S. E., Arnett, W. D. & Clayton, D. D. The explosive burning of oxygen and silicon. *ApJS* **26**, 231+ (1973).
27. Amari, S. *et al.* Interstellar SiC with unusual isotopic compositions - Grains from a supernova? *ApJL* **394**, L43–L46 (1992).
28. Timmes, F. X. *et al.* The production of  $^{44}\text{Ti}$  and  $^{60}\text{Co}$  in supernovae. *ApJ* **464**, 332+ (1996).
29. Lai, D. K. *et al.* A unique star in the outer halo of the Milky Way. *ApJL* **697**, L63–L67 (2009).

30. de Plaa, J. *et al.* Constraining supernova models using the hot gas in clusters of galaxies. *A&A* **465**, 345–355 (2007).
31. The, L.-S. *et al.* Are  $^{44}\text{Ti}$ -producing supernovae exceptional? *A&A* **450**, 1037–1050 (2006).
32. Chan, K.-W. & Lingenfelter, R. E. Positrons from supernovae. *ApJ* **405**, 614–636 (1993).
33. Knödseder, J. *et al.* The all-sky distribution of 511 keV electron-positron annihilation emission. *A&A* **441**, 513–532 (2005).
34. Oke, J. B. *et al.* The Keck low-resolution imaging spectrometer. *PASP* **107**, 375–+ (1995).
35. Gal-Yam, A. *et al.* in *The Multicolored Landscape of Compact Objects and Their Explosive Origins* (eds di Salvo, T., Israel, G. L., Piersant, L., Burderi, L., Matt, G. *et al.*) 297–303 (IOP Insitute of physics publishing LTD, 2007).
36. Oke, J. B. & Gunn, J. E. An efficient low resolution and moderate resolution spectrograph for the Hale telescope. *PASP* **94**, 586–+ (1982).
37. Chu, Y.-H. & Gruendl, R. A. in *Massive Star Formation: Observations Confront Theory* (eds Beuther, H., Linz, H. & Henning, T.) 415–+ (ASP, 2008).
38. Schilbach, E. & Röser, S. On the origin of field O-type stars. *A&A* **489**, 105–114 (2008).
39. Anderson, J. P. & James, P. A. Constraints on core-collapse supernova progenitors from correlations with  $\text{H}\alpha$  emission. *MNRAS* **390**, 1527–1538 (2008).
40. Dyson, J. E. & Hartquist, T. W. On the structure of intermediate- and high-velocity clouds. *MNRAS* **203**, 1233–1238 (1983).
41. Christodoulou, D. M., Tohline, J. E. & Keenan, F. P. Star-forming processes far from the galactic disk: inoperative or indolent where operative. *ApJ* **486**, 810–+ (1997).
42. Martos, M. *et al.* Spiral density wave shock-induced star formation at high galactic latitudes. *ApJL* **526**, L89–L92 (1999).
43. Heraudeau, P. & Simien, F. Optical and I-band surface photometry of spiral galaxies. I. The data. *AAPS* **118**, 111–155 (1996).
44. Kennicutt, Jr., R. C. & Kent, S. M. A survey of H-alpha emission in normal galaxies. *AJ* **88**, 1094–1107 (1983).
45. Soderberg, A. M. in *Supernova 1987A: 20 Years After: Supernovae and Gamma-Ray Bursters* (eds Immler, S., Weiler, K. & McCray, R.) 492–499 (IOP, 2007).

46. Howell, D. A. *et al.* Gemini spectroscopy of supernovae from the supernova legacy survey: Improving high-redshift supernova selection and classification. *ApJ* **634**, 1190–1201 (2005).
47. Hamuy, M. *et al.* Optical and infrared spectroscopy of SN 1999ee and SN 1999ex. *AJ* **124**, 417–429 (2002).
48. Filippenko, A. V. & Sargent, W. L. W. The unique supernova (1985f) in NGC 4618. *AJ* **91**, 691–696 (1986).
49. Gaskell, C. M. *et al.* Type Ib supernovae 1983n and 1985f - Oxygen-rich late time spectra. *ApJL* **306**, L77–L80 (1986).
50. Arnett, W. D. Type I supernovae. I - Analytic solutions for the early part of the light curve. *ApJ* **253**, 785–797 (1982).
51. Stehle, M. *et al.* Abundance stratification in Type Ia supernovae - I. The case of SN 2002bo. *MNRAS* **360**, 1231–1243 (2005).
52. Modjaz, M. *et al.* From shock breakout to peak and beyond: Extensive panchromatic observations of the aspherical type Ib supernova 2008D associated with Swift X-ray transient 080109. *ArXiv* **0805.2201**, (2008).
53. Valenti, S. *et al.* The broad-lined type Ic supernova 2003jd. *MNRAS* **383**, 1485–1500 (2008).
54. NED *Nasa/ipac extragalactic database* <http://nedwww.ipac.caltech.edu/>.
55. Blaauw, A. On the origin of the O- and B-type stars with high velocities (the "run-away" stars), and some related problems. *Bulletin of the Astronomical Institutes of the Netherlands* **15**, 265–+ (1961).
56. Hoogerwerf, R., de Bruijne, J. H. J. & de Zeeuw, P. T. On the origin of the O and B-type stars with high velocities. II. Runaway stars and pulsars ejected from the nearby young stellar groups. *A&A* **365**, 49–77 (2001).
57. Hills, J. G. Hyper-velocity and tidal stars from binaries disrupted by a massive Galactic black hole. *Nature* **331**, 687–689 (1988).
58. Brown, W. R. *et al.* Discovery of an unbound hypervelocity star in the Milky Way halo. *ApJL* **622**, L33–L36 (2005).
59. Edelmann, H. *et al.* HE 0437-5439: An unbound hypervelocity main-sequence B-Type star. *ApJL* **634**, L181–L184 (2005).

60. Hirsch, H. A. *et al.* US 708 - an unbound hyper-velocity subluminal O star. *A&A* **444**, L61–L64 (2005).
61. Eisenhauer, F. *et al.* SINFONI in the Galactic center: Young stars and infrared flares in the central light-month. *ApJ* **628**, 246–259 (2005).
62. Ghez, A. M. *et al.* Stellar orbits around the Galactic center black hole. *ApJ* **620**, 744–757 (2005).
63. Miyamoto, M. & Nagai, R. Three-dimensional models for the distribution of mass in galaxies. *Publ. of the Astronomical Society of Japan* **27**, 533–543 (1975).
64. Shankar, F. *et al.* New relationships between galaxy properties and host halo mass, and the role of feedbacks in galaxy formation. *ApJ* **643**, 14–25 (2006).
65. Gorgas, J., Jablonka, P. & Goudfrooij, P. Stellar population gradients in bulges along the Hubble sequence. I. The data. *A&A* **474**, 1081–1092 (2007).
66. Leonard, P. J. T. The maximum possible velocity of dynamically ejected runaway stars. *AJ* **101**, 562–571 (1991).
67. Leonard, P. J. T. & Duncan, M. J. Runaway stars from young star clusters containing initial binaries. II - A mass spectrum and a binary energy spectrum. *AJ* **99**, 608–616 (1990).
68. Ferrarese, L. & Merritt, D. A fundamental relation between supermassive black holes and their host galaxies. *ApJL* **539**, L9–L12 (2000).
69. Gebhardt, K. *et al.* A relationship between nuclear black hole mass and galaxy velocity dispersion. *ApJL* **539**, L13–L16 (2000).
70. Hills, J. G. Computer simulations of encounters between massive black holes and binaries. *AJ* **102**, 704–715 (1991).
71. Bromley, B. C. *et al.* Hypervelocity stars: Predicting the spectrum of ejection velocities. *ApJ* **653**, 1194–1202 (2006).
72. Abt, H. A. Normal and abnormal binary frequencies. *ARAA* **21**, 343–372 (1983).
73. Morrell, N. & Levato, H. Spectroscopic binaries in the Orion OB1 association. *ApJS* **75**, 965–985 (1991).
74. Kobulnicky, H. A. & Fryer, C. L. A new look at the binary characteristics of massive stars. *ApJ* **670**, 747–765 (2007).

75. Perets, H. B. Runaway and hypervelocity stars in the Galactic halo: Binary rejuvenation and triple disruption. *ApJ*, *in press* **ArXiv:0802.1004**, (2008).
76. Heber, U. *et al.* The B-type giant HD 271791 in the Galactic halo. Linking run-away stars to hyper-velocity stars. *A&A* **483**, L21–L24 (2008).
77. Yu, Q. & Tremaine, S. Ejection of Hypervelocity Stars by the (Binary) Black Hole in the Galactic Center. *ApJ* **599**, 1129–1138 (2003).
78. Perets, H. B., Hopman, C. & Alexander, T. Massive Perturber-driven Interactions between Stars and a Massive Black Hole. *ApJ* **656**, 709–720 (2007).
79. Perets, H. B. Dynamical and evolutionary constraints on the nature and origin of hyper-velocity stars. *ApJ* **690**, 795–801 (2009).
80. Perets, H. B. *et al.* Dynamical evolution of the young stars in the Galactic center: N-body simulations of the S-stars. *ArXiv* **0903.2912**, (2009).
81. Gould, A. & Quillen, A. C. Sagittarius A\* Companion S0-2: A Probe of Very High Mass Star Formation. *ApJ* **592**, 935–940 (2003).
82. Gillessen, S. *et al.* Monitoring Stellar Orbits Around the Massive Black Hole in the Galactic Center. *ApJ* **692**, 1075–1109 (2009).
83. Puckett, T. & Dowdle, G. Supernova 2000ds in NGC 2768. *IAU Circulars* **7507**, 2–+ (2000).
84. Aazami, A. B. & Li, W. D. Supernova 2001co in NGC 5559. *IAU Circulars* **7643**, 2–+ (2001).
85. Graham, J., Li, W., Puckett, T., Toth, D. & Qiu, Y. L. Supernovae 2003E, 2003F, 2003G, 2003H. *IAU Circulars* **8045**, 1–+ (2003).
86. Pugh, H. & Li, W. Supernova 2003dg in UGC 6934. *IAU Circulars* **8113**, 2–+ (2003).
87. Puckett, T., Toth, D., Schwartz, M., Holvorcem, P. R., Wood-Vasey, W. M. *et al.* Supernovae 2003dm, 2003dn, 2003do, 2003dp, 2003dq, 2003dr. *IAU Circulars* **8117**, 1–+ (2003).
88. Graham, J., Li, W., Schwartz, M. & Trondal, O. Supernovae 2004gw, 2005B, 2005D, 2005E, 2005F, 2005G. *IAU Circulars* **8465**, 1–+ (2005).
89. Chu, J. & Li, W. Supernova 2007ke in NGC 1129. *Central Bureau Electronic Telegrams* **1084**, 1–+ (2007).

90. Ravindranath, S. *et al.* Central structural parameters of early-type galaxies as viewed with Nicmos on the Hubble space telescope. *AJ* **122**, 653–678 (2001).
  91. Kauffmann, G. *et al.* The host galaxies of active galactic nuclei. *MNRAS* **346**, 1055–1077 (2003).
  92. Sauer, D. N. *et al.* The properties of the ‘standard’ Type Ic supernova 1994I from spectral models. *MNRAS* **369**, 1939–1948 (2006).
  93. Mazzali, P. A., Iwamoto, K. & Nomoto, K. A spectroscopic analysis of the energetic type Ic Hypernova SN 1997EF. *ApJ* **545**, 407–419 (2000).
  94. Tominaga, N. *et al.* The unique type Ib supernova 2005bf: A WN star explosion model for peculiar light curves and spectra. *ApJL* **633**, L97–L100 (2005).
  95. Li, L.-X. Correlation between the peak spectral energy of gamma-ray bursts and the peak luminosity of the underlying supernovae: implication for the nature of the gamma-ray burst-supernova connection. *MNRAS* **372**, 1357–1365 (2006).
  96. Mazzali, P. A. *et al.* The aspherical properties of the energetic type Ic SN 2002ap as inferred from its nebular spectra. *ApJ* **670**, 592–599 (2007).
  97. Soderberg, A. M. *et al.* An HST study of the supernovae accompanying GRB 040924 and GRB 041006. *ApJ* **636**, 391–399 (2006).
  98. Nadyozhin, D. K. Explosion energies, nickel masses and distances of type II plateau supernovae. *MNRAS* **346**, 97–104 (2003).
  99. Zampieri, L. in *1604-2004: Supernovae as Cosmological Lighthouses* (eds Turatto, M., Benetti, S., Zampieri, L. & Shea, W.) 358–+ (ASP, 2005).
  100. Li, W. *et al.* SN 2002cx: The most peculiar known type Ia supernova. *PASP* **115**, 453–473 (2003).
  101. Jha, S. *et al.* Late-time spectroscopy of SN 2002cx: The prototype of a new subclass of type Ia supernovae. *AJ* **132**, 189–196 (2006).
-